PAPER

Decoherence: a numerical study

To cite this article: Chris Nagele et al 2023 J. Phys. A: Math. Theor. 56 085301

View the article online for updates and enhancements.

You may also like

- Nonequilibrium distribution functions in electron transport: decoherence, energy redistribution and dissipation
 Thomas Stegmann, Orsolya Ujsághy and Dietrich E Wolf
- Quantum many-body theory for electron spin decoherence in nanoscale nuclear spin baths
 Wen Yang, Wen-Long Ma and Ren-Bao
- Open-system dynamics of entanglement:a key issues review Leandro Aolita, Fernando de Melo and Luiz Davidovich

Decoherence: a numerical study

Chris Nagele¹, Oliver Janssen^{2,3,4,*} and Matthew Kleban²

- Department of Astronomy, Graduate School of Science, The University of Tokyo, Tokyo 113-0033, Japan
- ² Center for Cosmology and Particle Physics, New York University, 726 Broadway, New York, NY 10003, United States of America
- ³ International Centre for Theoretical Physics, Strada Costiera 11, 34151 Trieste, Italy
- ⁴ Institute for Fundamental Physics of the Universe, Via Beirut 2, 34014 Trieste, Italy

E-mail: ojanssen@ictp.it

Received 28 January 2022; revised 3 November 2022 Accepted for publication 6 February 2023 Published 16 February 2023



Abstract

We study quantum decoherence numerically in a system consisting of a relativistic quantum field theory coupled to a measuring device that is itself coupled to an environment. The measuring device and environment are treated as quantum, non-relativistic particles. We solve the Schrödinger equation for the wave function of this tripartite system using exact diagonalization. Although computational limitations on the size of the Hilbert space prevent us from exploring the regime where the device and environment consist of a truly macroscopic number of degrees of freedom, we nevertheless see clear evidence of decoherence: after tracing out the environment, the density matrix describing the system and measuring device evolves quickly towards a matrix that is close to diagonal in a subspace of pointer states. We measure the speed with which decoherence spreads in the relativistic quantum field theory for a range of parameters. We find that it is less than the speed of light but faster than the speed of the massive charges in the initial state.

Keywords: decoherence, relativistic quantum field theory, environment-induced superselection, spread of decoherence in a relativistic theory

(Some figures may appear in colour only in the online journal)

1. Introduction

Quantum mechanics is the most successful theory in the history of science. It explains phenomena as disparate as fluorescent lights, nuclear reactions and the origin of structure in the

^{*} Author to whom any correspondence should be addressed.

Universe, and is precise enough to calculate the magnetic moment of the electron to 12 significant figures. Despite these extraordinary successes, certain fundamental features of the theory remain obscure. Chief among them is the question of how quantum mechanics relates to the classical world—how (or if) the Born rule for calculating the probabilities of measurement results from the quantum wave function should be understood, why classical (rather than quantum) physics accurately describes the macroscopic world and how to understand the apparent collapse of the wave function following a measurement.

A widely-accepted idea that bears on these mysteries is decoherence [1–7] (for reviews see [8–10]). The idea is that the interaction of a microscopic quantum system with a macroscopic measuring device (or 'apparatus') and an environment should, via Schrödinger time evolution, cause the wave function to evolve towards a specific form. Suppose the initial quantum state of the system was a superposition of eigenstates of the operator being measured that is unentangled with the environment and apparatus. The measurement process should generate entanglement such that after tracing out the environment, the final wave function will approximate a mixed state that is a sum over eigenstates times appropriate states of the apparatus, weighted by the Born-rule probabilities. For all observables restricted to the systemapparatus subspace, this mixed state gives predictions that are precisely identical to a *classical* probabilistic mixture of these pure quantum eigenstates with the Born-rule probabilities (see section 2)—just what traditional interpretations predict following the interaction of the system with a measuring device [11]. Hence, if this evolution takes place it can be regarded as at least a partial explanation for wave function collapse with the correct probabilities. Unfortunately, the difficulties inherent in solving for the time evolution of the quantum state of macroscopic systems make it very difficult to establish whether this is the case.

In this paper we make two novel contributions. First, we define a metric that quantifies the degree of decoherence. Our metric can be applied to any tripartite quantum system (system, measuring apparatus and environment) that can be interpreted as making a measurement on some initial state. The metric is the distance between two density matrices. The first matrix ρ is the state resulting from tracing over the environment after the measurement has taken place. The second matrix ρ_D is a sum of individual density matrices weighted by normalized probabilities, where each individual matrix is the result of time evolution and tracing over the environment for a specific initial state in the pointer basis. (We take the pointer basis to denote the collection of product states of the system and the measuring apparatus which persist despite the interaction with the environment. These apparatus states can be viewed as records of the corresponding state of the system. Usually only the apparatus part of these states is referred to as the pointer basis, but we choose not to do this.) For example, if the apparatus is designed to measure the spin along z of a qubit, ρ_D is the weighted sum of the density matrices corresponding to initial states that are spin z eigenstates times the corresponding apparatus states, with weights that are the squared amplitudes of the actual initial state expanded in this basis. The idea is that ρ_D corresponds to a projective measurement in the Copenhagen interpretation (because there is no interference between the terms in the sum). The closer ρ is to ρ_D , the more decoherence due to the environment has removed off-diagonal terms (in the pointer basis).

Our second contribution is to define and measure the 'speed of decoherence'—the speed with which decoherence spreads across a relativistic system. This requires a system with a sufficiently large size, which in turn necessitates a large Hilbert space. Because we use exact diagonalization (a numerical technique that evolves the system exactly but requires computational resources that scale exponentially with Hilbert space dimension), this forces us to sharply restrict the size of the Hilbert spaces of the apparatus and environment. Nevertheless, our metric shows that the system still decoheres substantially. (We note that our metric on

decoherence could be applied to a more traditional setup where the system is much smaller than the apparatus and environment.)

The system we study is an interacting, relativistic quantum field theory (QFT)—the massive Schwinger model, or quantum electrodynamics (QED) defined in one space and one time dimension. The QFT is coupled to a measuring device or 'apparatus' (modeled as a heavy quantum particle) via a von Neumann-type interaction. The apparatus reacts to the presence of charges at a particular location in the Schwinger system. The apparatus is in turn coupled to an environment. We take the environment to be a light particle that interacts with the apparatus via a local (in position) interaction potential. We think of this light particle as a molecule of gas that the experimenter failed to evacuate from the tube containing the apparatus. After solving the Schrödinger equation for the full tripartite system, we trace over the environment to produce a density matrix for the system plus apparatus, and compare the resulting mixed state to the one predicted by decoherence.

There are several limitations to our study. Our system, apparatus, and environment are oversimplified. A real apparatus might interact with $\sim 10^{24}$ air molecules; our study includes 10^0 air molecules. The continuum Schwinger system is relativistic and local; our discretized version only has these properties at large number of lattice sites N. We investigate the convergence as $N \to \infty$, but due to numerical limitations are unable to extrapolate very far.

The advantage of our approach is that we make no approximations apart from numerical discretization, nor do we assume anything about the interpretation of quantum mechanics or the Born rule. Instead, we simply evolve the wave function and compare it to the one predicted by the theory of decoherence. Furthermore (in contrast to the toy examples usually studied in this context) the system being measured is a causal, relativistic QFT that is similar in many ways to the QFTs believed to describe the fundamental physics of our world. This opens the door to investigating *causal* aspects of decoherence, such as how localized measures of decoherence spread in spacetime.

2. Background and previous work

The basic formalism of decoherence (see e.g. [9]) takes place in a tripartite Hilbert space \mathcal{H} consisting of the subsystems \mathcal{S} (the system), \mathcal{A} (the apparatus) and \mathcal{E} (the environment): $\mathcal{H} = \mathcal{H}_{\mathcal{S}} \otimes \mathcal{H}_{\mathcal{A}} \otimes \mathcal{H}_{\mathcal{E}}$. An idealized version of decoherence would be a pure state $|\psi\rangle \in \mathcal{H}$ that evolves from a separable to an entangled form in the following way under the Schrödinger equation as the system interacts with the apparatus:

$$|\psi(0)\rangle = \left(\sum_{n} c_{n} |s_{n}\rangle\right) |a_{0}\rangle |e_{0}\rangle \xrightarrow{(1)} \left(\sum_{n} c_{n} |s_{n}\rangle |a_{n}(t_{1})\rangle\right) |e_{0}\rangle$$

$$\xrightarrow{(2)} \left(\sum_{n} c_{n} |s_{n}\rangle |a_{n}(t)\rangle |e_{n}(t)\rangle\right) = |\psi(t)\rangle \quad (1)$$

where $0 < t_1 < t$. The arrows represent an idealized evolution in the time intervals $[0,t_1]$ and $[t_1,t]$, respectively. To achieve such a dynamics we must assume, firstly, that the interaction Hamiltonian dominates the time evolution of $|\psi\rangle$. Then, we assume the part of the interaction Hamiltonian that couples $\mathcal S$ with $\mathcal A$, and the $\mathcal S$ states $|s_n\rangle$, are such that the $|s_n\rangle$ are left invariant up to a multiplicative factor (similarly for the apparatus-environment interaction Hamiltonian and the apparatus states $|a_n(t)\rangle$). We also assume there are two time scales, one for the interaction between the system and the apparatus and another for the interaction between the apparatus and the environment, and that these interactions may be thought of as happening

successively. In a realistic setup all of these assumptions will be broken to some extent. As reviewed below in general one searches for apparatus states which best retain correlations with the system over time.

By definition, we do not measure properties of the environment and so it should be traced out. This leads to the following reduced density matrix for the \mathcal{SA} subsystem:

$$\rho_{\mathcal{SA}}(t) = \text{Tr}_{\mathcal{E}} |\psi(t)\rangle \langle \psi(t)|$$

$$= \sum_{n,m} c_n c_m^* \langle e_m(t) | e_n(t) \rangle |s_n\rangle |a_n(t)\rangle \langle s_m |\langle a_m(t) |.$$
(2)

A key mathematical claim of decoherence is that the environment states $\{|e_n(t)\rangle\}$ will rapidly become orthogonal to each other so that $\langle e_m(t)|e_n(t)\rangle \to \delta_{m,n}$. Then

$$\rho_{\mathcal{SA}}(t) \to \sum_{n} |c_n|^2 |s_n\rangle |a_n(t)\rangle \langle s_n| \langle a_n(t)|. \tag{3}$$

We call the collection of states $\{|s_n\rangle|a_n(t)\rangle\}\subset\mathcal{H}_{\mathcal{S}}\otimes\mathcal{H}_{\mathcal{A}}$ 'pointer states': they retain their correlation despite an interaction with the environment⁵. Equation (3) indicates that $\rho_{\mathcal{S}\mathcal{A}}(t)$ becomes diagonal in (a subset of) pointer states⁶. The interaction with the environment has suppressed interference terms of the type $|s_n\rangle|a_n(t)\rangle\langle s_m|\langle a_m(t)|, m\neq n$, that would have been present in the $\mathcal{S}\mathcal{A}$ density matrix had \mathcal{A} not been coupled to \mathcal{E} .

However, in realistic systems all states become entangled with the environment at some level. This means no state will remain pure after tracing over \mathcal{E} . Given this, one way to characterize pointer states is the 'predictability sieve' [13]. Given an initial state $|\chi_0\rangle = |s\rangle|a\rangle \in \mathcal{H}_{\mathcal{S}} \otimes \mathcal{H}_{\mathcal{A}}$ and a typical environment state $|e_r\rangle$, we can consider the entropy of the reduced density matrix $\rho_{\mathcal{S}\mathcal{A}}(t) = \text{Tr}_{\mathcal{E}}|\psi(t)\rangle\langle\psi(t)|, S(t) = -\text{Tr}_{\mathcal{S}\mathcal{A}}\left(\rho_{\mathcal{S}\mathcal{A}}\log\rho_{\mathcal{S}\mathcal{A}}\right)$, where $|\psi(t)\rangle$ is the time evolution of the initial state $|\chi_0\rangle|e_r\rangle$. Pointer states are those $|\chi_0\rangle$ for which S(t) rises slowly on timescales typical of the dynamics of \mathcal{S} and \mathcal{A} .

Experiments conducted on the system and apparatus only cannot distinguish the mixed state (3) from a classical statistical ensemble of quantum states $\{|s_n\rangle|a_n(t)\rangle\}$ with probabilities $|c_n|^2$ [14]. To see this, note that for any observable \mathcal{O} , using (3) we have

$$\langle \mathcal{O} \rangle = \operatorname{Tr}_{\mathcal{S}\mathcal{A}} \left[\mathcal{O} \rho_{\mathcal{S}\mathcal{A}}(t) \right] = \sum_{n} |c_{n}|^{2} \langle s_{n} | \langle a_{n}(t) | \mathcal{O} | s_{n} \rangle | a_{n}(t) \rangle,$$

$$(4)$$

which is manifestly identical to $\langle \mathcal{O} \rangle$ computed in the classical ensemble of quantum states mentioned above. This holds regardless of whether the states $|s_n\rangle|a_n(t)\rangle$ are orthogonal. Similarly, the convex combination of *mixed* states

$$\rho_D(t) = \sum_n |c_n|^2 \rho_n(t) \tag{5}$$

is equivalent in the same sense to a classical statistical ensemble of mixed states ρ_n with probabilities $|c_n|^2$. If the $\rho_n(t)$ are time-evolved pointer states (which, as just mentioned, will not in general remain pure), then $\rho_D(t)$ can be thought of as the state predicted by decoherence: a classical statistical ensemble of time-evolved pointer states.

⁵ As mentioned in the Introduction, we call the product states $|s_n\rangle|a_n(t)\rangle$ 'pointer states' in this paper, while in the literature this term usually refers to just the $|a_n(t)\rangle$ states.

⁶ The pointer states do not form a basis—generally they form an overcomplete set. E.g. in the case of a harmonic oscillator S coupled to a heat bath E, the pointer states are the coherent states of the harmonic oscillator, provided the friction constant of the environment is much smaller than the oscillator's frequency [12].

Despite the crucial role attributed to decoherence in understanding the relation of quantum mechanics to the classical world (see e.g. [7, 15–18]), analytical studies of it have been limited to specific interactions and toy models (see e.g. [19–21], and the review [10] and references therein), while the few numerical studies to date are limited by the computational cost of simulating exponentially large Hilbert spaces. One numerical study [22] considers two nonrelativistic particles interacting on an interval. The heavier of the two particles is taken as \mathcal{S} while the lighter is \mathcal{E} ; there is no \mathcal{A} . The authors consider the time evolution of an initial product state consisting of two Gaussian lumps in position space for the heavy particle that move towards each other, times a single Gaussian lump for the lighter particle. With no interaction, the position space probability density of the heavier particle $\mathcal S$ (obtained by tracing out the lighter particle \mathcal{E}) develops an interference pattern as the two lumps approach one another and overlap. With an appropriate interaction between the particles this inference pattern is destroyed: the heavy particle position space density is well-approximated by the sum of the two respective heavy particle densities even after they overlap. This is an example of the general decoherence mechanism described above applied to the specific observable $\mathcal{O} = x_{\text{heavy}}$ in equation (4), with the pointer states being the independent free time evolutions of the two heavy particle lumps.

In this work, we make no approximations (apart from those inherent in discretizing the system). For instance, the coupling between the apparatus and the environment is a realistic short-range interaction that would be difficult to analyze analytically, and our system S is an interacting relativistic QFT. Furthermore, we do not assume that the pointer states remain unentangled with the environment, and in fact all pointer states will become entangled—but more slowly than a typical state would (this is the predictability sieve criterion for pointer states described above). As a result, the sum over pure states in (4) must be replaced by the corresponding convex combination of density matrices (5) where the $\rho_n(t) \equiv \rho_{SA}(t)$ for $c_n = 1, c_{m \neq n} = 0$ (in other words, $\rho_n(t)$ is the density matrix resulting from tracing over the environment when the initial state is the single pointer state $|s_n\rangle|a_n(t)\rangle$). In the rest of this work, our primary measure of decoherence will be the distance between the density matrix $\rho_D(t)$ defined in (5) and the exact mixed state $\rho_{SA}(t)$ defined in (2).

There have been other studies of decoherence in relativistic QFT and quantum mechanics, e.g. [23–26]. To our knowledge, none have investigated the question of how fast decoherence spreads in the relativistic system after an interaction with the measuring device and environment.

3. Numerical methods and system

The quantum theory we study consists of three parts: an interacting relativistic QFT in one spatial dimension (\mathcal{S})—the massive Schwinger model—coupled via a von Neumann [27] type interaction to a massive, non-relativistic particle (the measuring device or apparatus \mathcal{A}) that is in turn coupled to a much lighter non-relativistic particle (the environment \mathcal{E}) via a local interaction in position space. We regard this light particle as an air molecule that our experimenter has failed to evacuate from the apparatus' cavity. This is the classic tripartite system-apparatus-environment theory considered in discussions of decoherence and reviewed in section 2.

The massive Schwinger model is QED in one space and one time dimension and is described by the Hamiltonian (in natural units)

$$\mathcal{H} = \int dy \left[-i\bar{\psi}\gamma^{1} \left(\frac{d}{dy} + igA_{1} \right) \right] \psi + \bar{\psi}\psi + \frac{E^{2}}{2} \right]$$

Table 1. Numerical values of the model parameters we chose, whose dynamics are shown in figures 2–4. From top to bottom in the first column, we have the ratio of the Schwinger mass to charge, the Schwinger parameter $x = 1/(ga)^2$, the mass of the apparatus and environment particles, the coupling between the Schwinger subsystem and the apparatus, the coupling between the apparatus and the air molecule, and the width of the interaction between the apparatus and the environment. The second column shows the fiducial values. These have been chosen to optimize the decoherence measures we will discuss in section 4. The third column shows an order of magnitude range over which each fiducial value can be varied, while the others are held fixed, such that the Bures distance $d_B(\rho, \rho_D)$ still decreases by at least 0.1 within 500 units of time t/a. Three orders of magnitude on either side of each fiducial value were investigated. For parameters which can take on negative values, such as the couplings, the range is shown only for positive values, but a similar range applies to negative values.

| Parameter | Fiducial value | Range |
|------------------------------|---------------------|--------------------|
| m/g | 50 | $10^{-2} - 10^4$ |
| x | 50 | $10^{-2} - 10^2$ |
| $m_{\mathcal{A}}$ | 400 | $10^1 - 10^5$ |
| $m_{\mathcal{E}}$ | 15 | $10^{-2} - 10^4$ |
| $g_{\mathcal{S}\mathcal{A}}$ | 0.1 | $10^{-2} - 10^{0}$ |
| $g_{\mathcal{A}\mathcal{E}}$ | -0.1 | $10^{-1} - 10^2$ |
| σ | $1/N_{\mathcal{S}}$ | $10^{-3} - 10^0$ |

where the electrons have mass m and charge g and interact via the electric fields E they produce, with vector potential A_1 . In contrast to QED in higher dimensions the electric field is non-dynamical, being determined entirely by the configuration of charges, and there are no magnetic fields. The theory is characterized by the dimensionless parameter m/g. For a fiducial value we choose m/g = 50 that is in the weakly interacting regime of the theory, but decoherence occurs for a wide range (including the strongly coupled regime $m/g \ll 1$, cf table 1).

The Schwinger model can be discretized on a so-called staggered lattice with spacing a, with electrons on even sites and positrons on odd sites. Using a Jordan–Wigner transformation, the discretized Hamiltonian is mapped to a spin system [28]

$$\begin{split} H_{\mathcal{S}} &= \frac{1}{g^2 a^2} \sum_{n=1}^{N-1} [\sigma_n^+ \sigma_{n+1}^- + \sigma_n^- \sigma_{n+1}^+] + \frac{N^2}{8} + N \frac{F}{g} \left(\frac{F}{g} - \frac{1}{2} \right) \\ &+ \frac{1}{4} \sum_{n=1}^{N} \left[n - N + (-1)^n \left(\frac{4m}{g^2 a} + \frac{1}{2} \right) - \frac{1}{2} \right] \sigma_n^z \\ &+ \sum_{n=1}^{N-1} (N-n) \left[\frac{F}{g} \sigma_n^z + \frac{1}{2} \sum_{l < n} \sigma_l^z \sigma_n^z \right] \end{split}$$

where *N* is the total number of Schwinger sites, σ^{\pm} are the Pauli matrices, and *F* is the initial electric field (for a more detailed description, see [29]).

The Hamiltonians for the apparatus and environment are those of massive free non-relativistic particles:

$$H_{\mathcal{A}} = \frac{p_{\mathcal{A}}^2}{2m_{\mathcal{A}}}, \ H_{\mathcal{E}} = \frac{p_{\mathcal{E}}^2}{2m_{\mathcal{E}}}$$

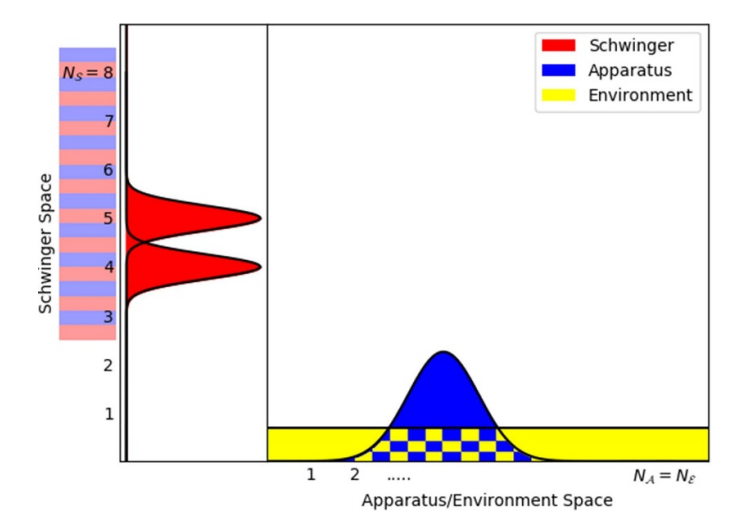


Figure 1. Schematic showing the massive Schwinger quantum field theory (vertical axis) and the charge density for a particle-anti particle pair (red). The horizontal axis shows the position-space density of the apparatus (heavy particle, blue) and environment (light particle, yellow). The apparatus is coupled to the charge density of the Schwinger system at all but the bottom two sites 1 and 2, and the apparatus and environment are coupled via a local (in position) interaction potential (cross-hatching indicates where the initial state wave functions overlap). We choose a uniform initial state for the environment particle to mimic a generic state of many environment particles in a more realistic setup.

where p is the momentum operator and m is the mass. The interaction Hamiltonian between the Schwinger system and the apparatus takes the form

$$H_{\mathcal{S}\mathcal{A}} = g_{\mathcal{S}\mathcal{A}} \left[\left(C_{\text{top}} - \langle \Omega |_{\mathcal{S}} C_{\text{top}} | \Omega \rangle_{\mathcal{S}} \mathbb{1}_{\mathcal{S}} \right) \otimes p_{\mathcal{A}} \right]$$
 (6)

where $g_{\mathcal{S}\mathcal{A}}$ is a (positive) coupling constant, $|\Omega\rangle_{\mathcal{S}}$ is the ground state of the Schwinger Hamiltonian, and C_{top} is the fermion density averaged over all but the bottom two Schwinger lattice sites. This interaction will cause the apparatus to move to the right in figure 1 (towards larger values of the apparatus position $x_{\mathcal{A}}$) when charges are present at any site except the bottom two of the Schwinger system. We subtract $\langle \Omega|_{\mathcal{S}}C_{\text{top}}|\Omega\rangle_{\mathcal{S}}\mathbb{1}_{\mathcal{S}}$ so that the apparatus is calibrated to react as little as possible in the ground state. A state with charges initially at sites 1 and 2 however will develop support on the higher sites after some time and start interacting with the apparatus. This specific interaction is tailored to illustrate decoherence in the linear combination of (ground state)+(state with charges at sites 1 and 2), as we discuss in detail in section 4.

Lastly, the interaction between the apparatus and the environment is short-range and local (in position space)

$$H_{A\mathcal{E}} = g_{A\mathcal{E}} V(x_A \otimes \mathbb{1}_{\mathcal{E}} - \mathbb{1}_A \otimes x_{\mathcal{E}})$$

where $g_{\mathcal{A}\mathcal{E}}$ is the coupling, $x_{\mathcal{A}}$, $x_{\mathcal{E}}$ are the position operators for the apparatus and environment particles, and V is the interaction potential that we take to be Gaussian,

$$V(x) = \frac{1}{\sqrt{2\pi}\sigma} \exp\left(\frac{-x^2}{2\sigma^2}\right),\,$$

where σ is the range of the interaction.

For simplicity and because the interaction is local in position, the number of lattice sites for the apparatus and environment are equal, $N_A = N_E$ (taken between 11 and 23 in our simulations of the dynamics, cf figure 4). The number of Schwinger sites is N_S (= 8 in our simulations). The full Hamiltonian reads

$$H = (H_{\mathcal{S}} \otimes \mathbb{1}_{\mathcal{A}} + H_{\mathcal{S}\mathcal{A}}) \otimes \mathbb{1}_{\mathcal{E}} + \mathbb{1}_{\mathcal{S}} \otimes (H_{\mathcal{A}} \otimes \mathbb{1}_{\mathcal{E}} + \mathbb{1}_{\mathcal{A}} \otimes H_{\mathcal{E}} + H_{\mathcal{A}\mathcal{E}}) .$$

Once computed, the Hamiltonian is diagonalized using NUMPY's eigh function which uses a divide and conquer algorithm in LAPACK, and the state at arbitrary time can then be easily calculated from any given initial state [29]. The numerical values of the parameters we chose to simulate the dynamics are detailed in table 1, as is the range over which our results are qualitatively unchanged.

4. Pointer states and numerical measures of decoherence

As mentioned above, decoherence is defined by the time evolution of the density matrix describing the system or the system and apparatus, after tracing over the environment. It refers to the tendency of the density matrix to become diagonal in a special basis of so-called 'pointer states' that depend on the details of the system and its interactions with the environment.

Given the form of the interactions, we expect the pointer states to be localized in the position basis for the apparatus, and to be (close to) charge eigenstates for the Schwinger system. The wave function of true position eigenstates would spread out more rapidly than the characteristic timescales of the system, so we will consider Gaussian wave functions with a standard deviation that is small enough to distinguish between apparatus locations before and after a measurement, but large enough to prevent the wave function from immediately spreading.

Therefore we will consider an initial state of the form

$$|\psi(t=0)\rangle = 2^{-1/2}(|\Omega\rangle_{\mathcal{S}} + |C\rangle_{\mathcal{S}}) \otimes |0\rangle_{\mathcal{A}} \otimes |e\rangle_{\mathcal{E}}$$
(7)

where $|\Omega\rangle_{\mathcal{S}}$ is the Schwinger ground state, $|C\rangle_{\mathcal{S}}$ is the Schwinger state with charges at sites 1 and 2 (for details see [29]), $|0\rangle_{\mathcal{A}}$ is a Gaussian in position for the apparatus. We choose $|e\rangle_{\mathcal{E}}$ to be an environment state that is completely de-localized in position space, so that the air molecule is equally likely to be found anywhere on the interval⁷. For simplicity we focus just on these two pointer states and their equally weighted linear combination (7).

Due to the boundary conditions the charges in the Schwinger state $|C\rangle_S$ have an upward momentum initially, so after some time they move out of the bottom two sites and enter the region where the coupling to the apparatus is active⁸. In figure 2 we plot the evolution of the charge density and positions of the apparatus and environment.

We define $\rho(t) = \rho_{SA}(t)$ to be the mixed state resulting from the partial trace over \mathcal{E} of this initial state:

$$\rho(t) \equiv \text{Tr}_{\mathcal{E}}|\psi(t)\rangle\langle\psi(t)|,\tag{8}$$

and $\rho_{\Omega}(t), \rho_{C}(t)$ to be the mixed states when we choose the initial state of the system to be $|\Omega\rangle_{\mathcal{S}}\otimes|0\rangle_{\mathcal{A}}\otimes|e\rangle_{\mathcal{E}}, |C\rangle_{\mathcal{S}}\otimes|0\rangle_{\mathcal{A}}\otimes|e\rangle_{\mathcal{E}}$ respectively and trace over \mathcal{E} at time t.

⁷ We also experimented with random initial states for the air molecule and found little difference in the results.

⁸ We consider a state with two equal and opposite charges to avoid a background electric field that would exert a net force on the charges.

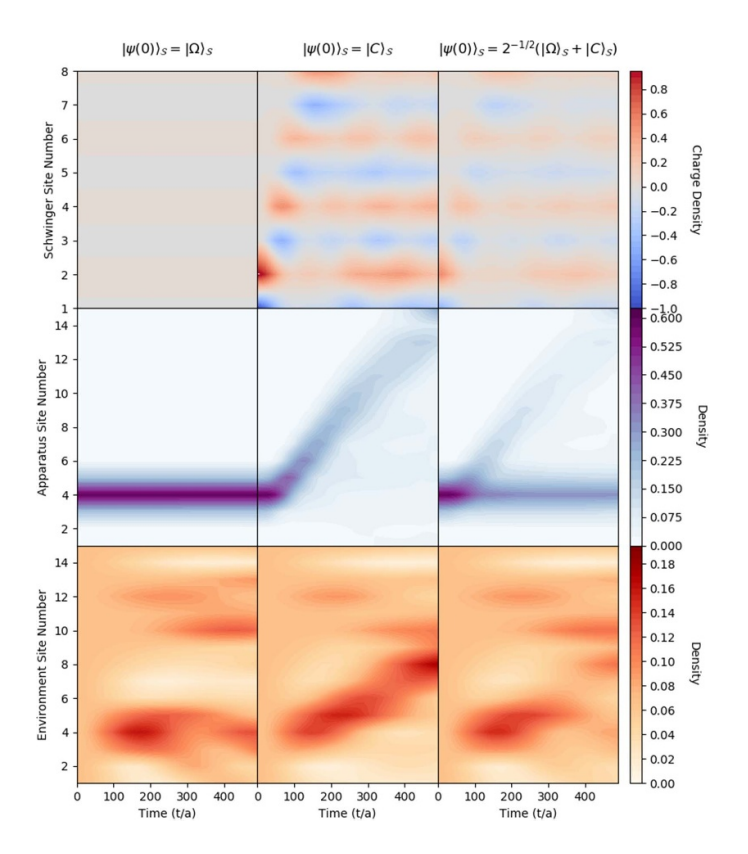


Figure 2. The expectation value of the charge density for the Schwinger model, the position of the apparatus, and the position of the environment (top, middle, and bottom rows) for three initial Schwinger states $|\Omega\rangle_{\mathcal{S}}, |C\rangle_{\mathcal{S}}$, and $2^{-1/2}(|\Omega\rangle_{\mathcal{S}} + |C\rangle_{\mathcal{S}})$ (cf (7)) (left, middle, and right columns).

As described above, the predictability sieve criterion for identifying pointer states quantitatively relies on the behavior of the entropy of entanglement with the environment. In a decohering system, the entropy of a pointer state should remain small (relative to a random state) for some time. To check whether we have indeed identified some pointer states correctly, we plot the von Neumann entanglement entropy of two such states vs. time and compare it to the entropy of a random state (see figure 3). The entropy indeed grows more slowly for our putative pointer states than for a random state.

As mentioned previously, our quantitative measure of decoherence will be the distance between the density matrix $\rho(t)$ (cf (8)) and

$$\rho_D(t) \equiv \frac{1}{2}\rho_{\Omega}(t) + \frac{1}{2}\rho_C(t). \tag{9}$$

If ρ and ρ_D are identical this would correspond to perfect decoherence, because it would mean that the system has evolved to a state that can be interpreted as a classical statistical ensemble of the two states it would have evolved to in each pointer state separately. Conversely, if they remain nearly as far apart as they are initially before the interaction, it would indicate that the system is not decohering.

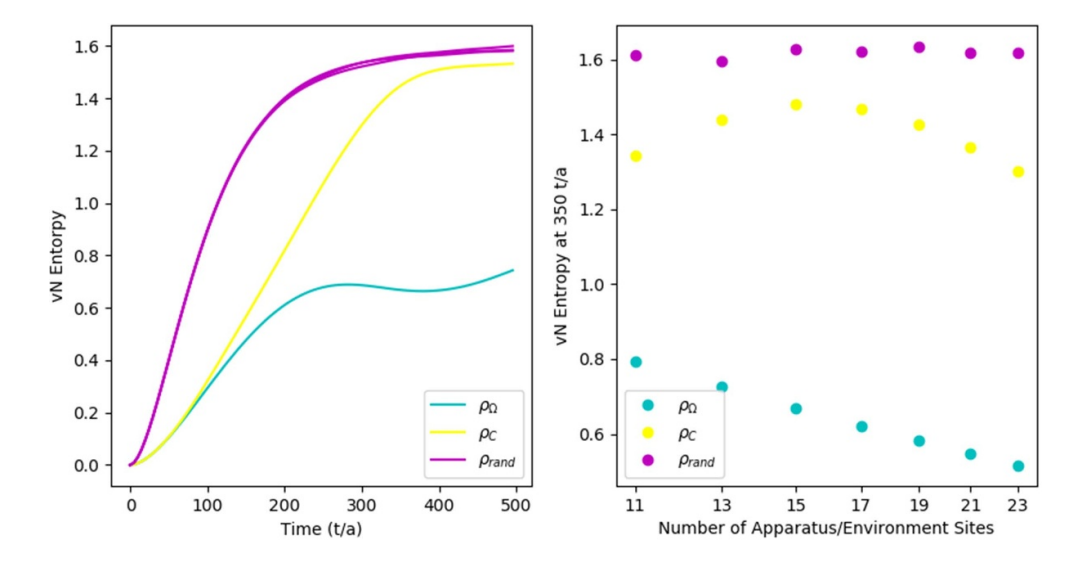


Figure 3. Left panel: time evolution of the von Neumann entropy of the mixed system+apparatus states $\rho_{\Omega}(t)$ and $\rho_{C}(t)$ obtained by the tracing over the environment of two putative initial pointer states $|\Omega\rangle_{\mathcal{S}}\otimes|0\rangle_{\mathcal{A}}$ and $|C\rangle_{\mathcal{S}}\otimes|0\rangle_{\mathcal{A}}$ (see (7) and (8)), compared to several randomly chosen states. Right panel: numerical stability of the left panel when increasing the size of the apparatus/environment Hilbert space.

There are several inequivalent definitions of distance between density matrices. We will use the Bures distance [30, 31]:

$$d_B(\rho_1,\rho_2) \equiv \sqrt{1-\sqrt{\text{Fid}(\rho_1,\rho_2)}} \equiv \sqrt{1-\text{Tr}\sqrt{\sqrt{\rho_1}\,\rho_2\sqrt{\rho_1}}}\,.$$

When ρ_1, ρ_2 are pure states $|\phi_1\rangle\langle\phi_1|, |\phi_2\rangle\langle\phi_2|$ the Bures distance reduces to the Fubini–Study distance $\sqrt{1-|\langle\phi_1,\phi_2\rangle|}$. In general [31, 32]

$$Fid(\rho_1, \rho_2) = \max_{|\psi_1\rangle, |\psi_2\rangle} |\langle \psi_1, \psi_2\rangle|^2,$$

where the maximum is taken over the set of all (independent) purifications $|\psi_{1,2}\rangle$ of $\rho_{1,2}$. The Bures distance is natural here since it involves the notion of purification, where density matrices are viewed as pure states of a larger Hilbert space. Note that we have normalized the Bures distance so that the maximal distance between two density matrices is $d_B = 1$ when the two density matrices have support on orthogonal subspaces, and $d_B = 0$ iff. $\rho_1 = \rho_2$.

5. Results

As we will now illustrate, the exact Schrödinger time evolution of the tripartite Schwinger-apparatus-environment quantum system indeed exhibits decoherence. Specifically, the distance $d_B(\rho(t), \rho_D(t))$ between the mixed state ρ obtained from tracing over the environment and the ideal decohered mixed state ρ_D evolves from its initial value to a substantially smaller value (we believe this minimum value would be even smaller if we were to increase the size

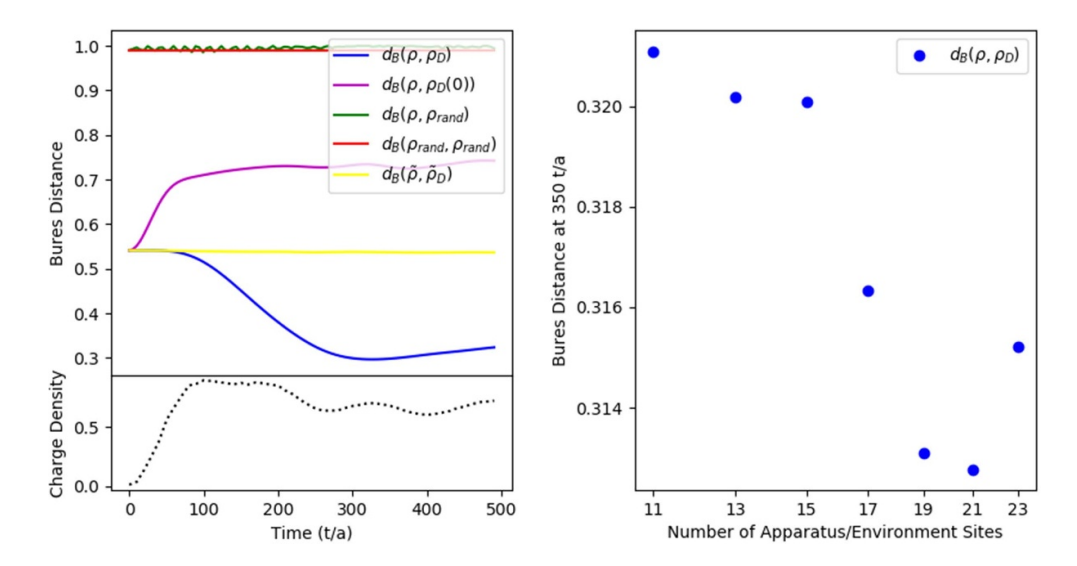


Figure 4. Left panel: Bures distance between the density matrix $\rho(t)$ obtained by tracing over the environment (8) and the fully decohered mixed state $\rho_D(t)$ (9) (blue). For comparison we plot the distance between $\rho(t)$ and a random state (green), the distance between two random states (red), the distance between $\rho(t)$ and $\rho(0)$ (magenta), and the distance between $\tilde{\rho}(t)$ and $\tilde{\rho}_D(t)$ (yellow), where $\tilde{\rho}, \tilde{\rho}_D$ are defined in the same way as ρ, ρ_D but relative to randomly chosen system-apparatus states (rather than pointer states). Left lower panel: average charge density of the top six Schwinger sites. Right panel: Bures distance $d_B(\rho, \rho_D)$ at a specific time (t/a = 350) as a function of the size of the apparatus and environment Hilbert spaces.

of the Hilbert space). As expected, this decrease begins when the system starts to interact with the apparatus (and the apparatus in turn interacts with the environment).

As a check, we also plot the distance between $\rho(t)$ and $\rho(0)$, between the analog of $\rho(t)$ and $\rho_D(t)$ where we replace the pointer states $|\Omega\rangle_{\mathcal{S}}\otimes|0\rangle_{\mathcal{A}}$ and $|C\rangle_{\mathcal{S}}\otimes|0\rangle_{\mathcal{A}}$ with random states, the distance between $\rho(t)$ and a random density matrix, and the distance between two random density matrices. None of these distances decrease with time, which establishes that the behavior we are observing is indeed consistent with the predictions of decoherence. These behaviors are illustrated in figures 2 and 4. The yellow line in 4—the Bures distance between $\tilde{\rho}(t)$ and $\tilde{\rho}(t)_D$, which are density matrices defined identically to ρ, ρ_D but relative to randomly chosen states rather than pointer states—exhibits no decrease over time. This illustrates that the system plus apparatus decoheres in the pointer basis selected by the interaction with the environment, but not in an arbitrary basis.

While we do not illustrate it in a figure, setting the apparatus-environment coupling $g_{\mathcal{A}\mathcal{E}}$ to zero also makes the Bures distance independent of time: $d_B(\rho(t), \rho_D(t)) = d_B(\rho(0), \rho_D(0))$. This is as expected from the theory of decoherence, because it is the time evolution of the environment states entangled with the system and apparatus that causes decoherence, and with $g_{\mathcal{A}\mathcal{E}} = 0$ no such entanglement is generated.

⁹ A random density matrix in $\mathcal{H}_{\mathcal{S}} \otimes \mathcal{H}_{\mathcal{A}}$ is chosen by acting with a random unitary (chosen according to the Haar measure) on a reference state in $\mathcal{H}_{\mathcal{S}} \otimes \mathcal{H}_{\mathcal{A}} \otimes \mathcal{H}_{\mathcal{E}}$ and tracing over $\mathcal{H}_{\mathcal{E}}$.

Our study is limited by the computational power of classical computers, which constrains us to consider far smaller Hilbert spaces than those that describe truly macroscopic measuring devices or environments (see e.g. [7]). This limitation is likely responsible for the fact that decoherence is only partially effective in our simulations (i.e. for the fact that the distance between the exact state ρ and the ideal decohered state ρ_D does not decrease to a value very close to zero). As an indication of what would happen with a larger Hilbert space, we investigated both the behavior of the von Neumann entropy of our putative pointer states after some time and the Bures distance between ρ and ρ_D as we increased the size of the apparatus and environment Hilbert spaces. Both results appear to show an increasing level of decoherence (figure 3).

6. Lorentz invariance and the speed of decoherence

An intriguing question that arises in thinking about decoherence and the 'splitting' of the wave function into classical branches is the question of when and where in spacetime these splits occur (see also [33]). This question is particularly interesting when the system under study is Lorentz invariant so that the spread of causal influences is limited by the speed of light. The Schwinger system we study is (in the continuum limit) invariant under 1+1-dimensional Lorentz transformations acting on time and the spatial direction it extends in. In our analysis the measuring apparatus and environment are represented by non-relativistic Hamiltonians. At first glance one might think that this will spoil the Lorentz invariance. However, if the interaction of the measuring device and apparatus with the Schwinger system is confined to a single location (or a small number of lattice sites) in the spatial direction of the Schwinger system, a measurement constitutes a *local* perturbation or source in the relativistic Schwinger system at this specific location. Therefore, in the continuum limit relativistic causality limits how rapidly the decoherence effects of a measurement can spread in the Schwinger direction.

To investigate this spread we studied an interaction Hamiltonian that is modified slightly relative to the rest of the paper: the Schwinger operator C_{top} (cf equation (6)) in this section is the fermion density averaged over only the top two lattice sites of the Schwinger system (as opposed to all but the bottom two). This makes the interaction more local (but does not qualitatively alter the results obtained in the rest of the paper).

To measure the spread of decoherence we define mixed states that are localized at some site *x* in the Schwinger space by tracing over the environment, the apparatus, and all the states associated with the Schwinger lattice sites except *x*:

$$\rho_x \equiv \mathsf{Tr}_{\mathcal{A}, \mathcal{S} \text{ sites } y \neq x}(\rho), \qquad \rho_{x,D} \equiv \mathsf{Tr}_{\mathcal{A}, \mathcal{S} \text{ sites } y \neq x}(\rho_D).$$

These localized mixed states are related to ρ , ρ_D (cf (8) and (9)) by the additional trace over all Schwinger sites $y \neq x$.

In figure 5 we plot the Bures distance between ρ_x and $\rho_{x,D}$. The difference is initially localized at the site of the charge. This is as expected: both the states $|\Omega\rangle_S$ and $|C\rangle_S$ are initially very close to the vacuum at the lattice sites away from the position of the charges, and hence are nearly identical. However, as the charges interact with the apparatus (and the apparatus with the environment) we see that the state ρ_x approaches the decohered state $\rho_{x,D}$ everywhere. In figure 6 we illustrate that for all the values of m/g we investigated, this decoherence spread happens at a speed that exceeds the speed of the charges, but that is slower than the speed of light (which is 1 site/unit time in figure 5). We leave further investigation of this phenomenon to future work.

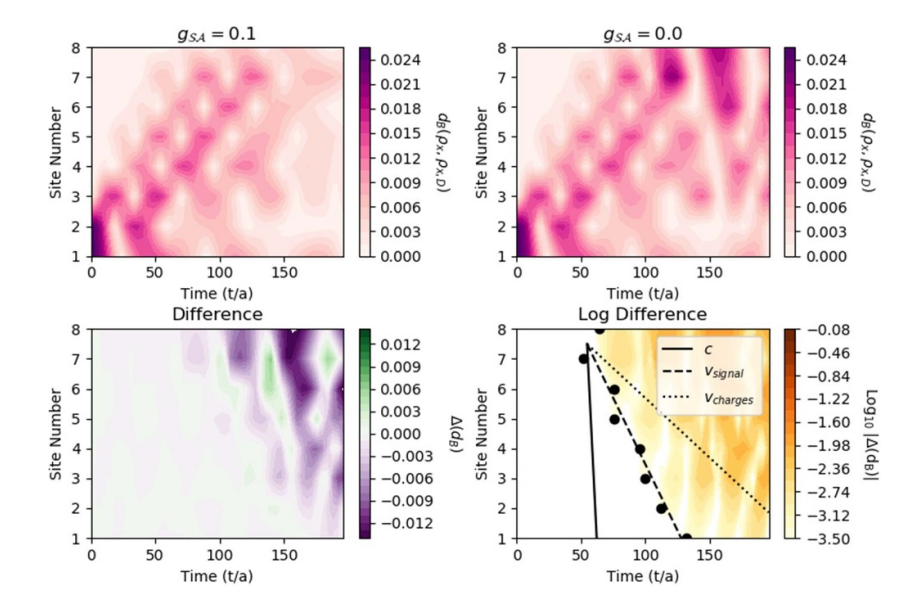


Figure 5. Top row: Bures distance between the local density matrix ρ_x and the fully decohered local matrix $\rho_{x,D}$, shown for zero and non-zero Schwinger-apparatus coupling. Bottom row: difference and log difference between the two plots in the top row. The speed of the charges v_{charges} is measured as they move upwards during the initial time period by two different methods, distance from the bottom to the top sites divided by the time the charge takes to traverse this distance, and a linear fit to spacetime points where the probability to observe a charge reaches a certain threshold. The speed of the spread of decoherence v_{signal} is determined by a fit to the points where the Bures distance between the decohered and un-decohered (non-interacting) states reaches a threshold and compared to c and the speed of the charges for reference.

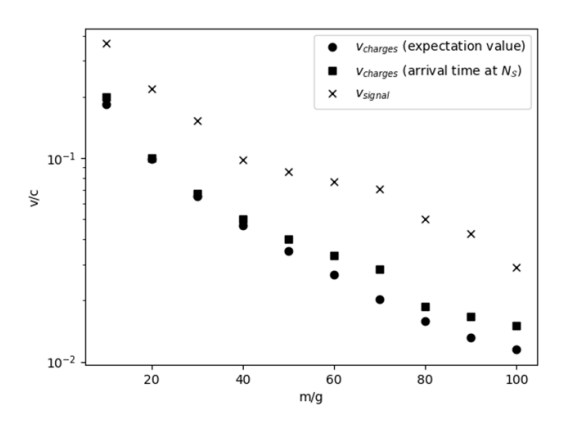


Figure 6. The speed of the charges and the speed of spread of decoherence as a function of $m g^{-1}$ (see the caption of figure 5 for an explanation of how the speeds are measured).

7. Conclusions

Our results illustrate that the exact quantum state of our model ρ , evolving in time according to the Schrödinger equation and with the environment traced over, indeed approaches the mixed

state ρ_D predicted by the theory of decoherence. In the sense that all expectation values are identical, ρ_D can be regarded as representing a classical statistical ensemble of quantum states with the probabilities predicted to follow a measurement in the conventional interpretations of quantum mechanics. In this sense our results bear directly on some of the central questions in the interpretation of the quantum wave function and the issue of measurement. Our study differs from previous work in that it is numerical, while most studies of decoherence have been analytic, and that we study an interacting relativistic QFT.

What we are testing is precise and quantitative: that the density matrix describing the system plus apparatus after tracing out the environment evolves towards a specific form that is defined relative to a specific set of pointer states. This is clearly a non-trivial claim that does not always hold. For instance—as we demonstrated explicitly—it does not hold if we choose a random set of pointer states rather than those that are selected out by the form of the interactions. This demonstrates that there cannot exist a general theorem or principle which imply our results for the collection of subsystems (which include a relativistic quantum field theory) that we are considering.

Perhaps the most intriguing result we have obtained is a measurement of the speed with which decoherence spreads in our relativistic system. It would be very interesting to investigate this speed further both numerically and analytically, and possibly connect it to studies of the speed of spread of entanglement (such as [34, 35]).

Data availability statement

All data that support the findings of this study are included within the article (and any supplementary files).

Acknowledgments

It is a pleasure to thank Aidan Chatwin-Davies, Jonathan Halliwell and Max Schlosshauer for useful comments on a draft of this paper. We also thank two anonymous referees for thorough and very useful feedback. The work of M K is supported by the NSF through the Grant PHY-1820814. O J acknowledges support from the Carl P Feinberg Graduate Fellowship.

ORCID iD

Oliver Janssen https://orcid.org/0000-0001-7911-9992

References

- [1] Zeh H 1970 On the interpretation of measurement in quantum theory Found. Phys. 1 69
- [2] Zeh H 1973 Toward a quantum theory of observation Found. Phys. 3 109
- [3] Zurek W H 1981 Pointer basis of quantum apparatus: Into what mixture does the wave packet collapse? Phys. Rev. D 24 1516
- [4] Zurek W H 1982 Environment-induced superselection rules Phys. Rev. D 26 1862
- [5] Caldeira A O and Leggett A J 1981 Influence of dissipation on quantum tunneling in macroscopic systems *Phys. Rev. Lett.* 46 211
- [6] Caldeira A and Leggett A 1983 Quantum tunnelling in a dissipative system Ann. Phys., NY 149 374
- [7] Joos E and Zeh H 1985 The emergence of classical properties through interaction with the environment Z. Phys. B 59 223
- [8] Zurek W H 2003 Decoherence, einselection and the quantum origins of the classical Rev. Mod. Phys. 75 715

- [9] Schlosshauer M 2004 Decoherence, the measurement problem and interpretations of quantum mechanics *Rev. Mod. Phys.* **76** 1267
- [10] Schlosshauer M 2019 Quantum decoherence Phys. Rep. 831 1
- [11] Dirac P 1958 The Principles of Quantum Mechanics (The International Series of Monographs on Physics) vol 27 (Oxford: Oxford University Press)
- [12] Paraoanu G-S 1999 Selection of squeezed states via decoherence Europhys. Lett. 47 279
- [13] Zurek W H 1994 Preferred observables, predictability, classicality, and the environment induced decoherence (arXiv:gr-qc/9402011)
- [14] Preskill J 2015 Lecture Notes on Quantum Information ch 2 (available at:www.theory.caltech.edu/people/preskill/ph229/)
- [15] Blanchard P, Giulini D, Joos E, Kiefer C, Kupsch J, Stamatescu I-O and Zeh H 1996 *Decoherence* and the Appearance of a Classical World in Quantum Theory (Berlin: Springer)
- [16] Breuer H-P and Petruccione F 2007 The Theory of Open Quantum Systems (Oxford: Oxford University Press)
- [17] Gell-Mann M and Hartle J B 2014 Adaptive coarse graining, environment, strong decoherence and quasiclassical realms *Phys. Rev.* A 89 052125
- [18] Gell-Mann M and Hartle J B 1993 Classical equations for quantum systems Phys. Rev. D 47 3345
- [19] Albrecht A 1992 Investigating decoherence in a simple system *Phys. Rev.* D 46 5504
- [20] Allahverdyan A E, Balian R and Nieuwenhuizen T M 2013 Understanding quantum measurement from the solution of dynamical models *Phys. Rep.* 525 1
- [21] Nieuwenhuizen T M, Perarnau-Llobet M and Balian R 2014 Lectures on dynamical models for quantum measurements Int. J. Mod. Phys. B 28 1430014
- [22] Adami R and Negulescu C 2012 A numerical study of quantum decoherence Commun. Comput. Phys. 12 85–108
- [23] Koksma J F, Prokopec T and Schmidt M G 2010 Decoherence in an interacting quantum field theory: the vacuum case Phys. Rev. D 81 065030
- [24] Giraud A and Serreau J 2010 Decoherence and thermalization of a pure quantum state in quantum field theory Phys. Rev. Lett. 104 230405
- [25] Cabrera R, Campos A G, Bondar D I and Rabitz H A 2016 Dirac open-quantum-system dynamics: formulations and simulations *Phys. Rev.* A **94** 052111
- [26] Chatterjee R and Majumdar A S 2017 Preservation of quantum coherence under Lorentz boost for narrow uncertainty wave packets *Phys. Rev.* A 96 052301
- [27] von Neumann J 1932 Mathematische Grundlagen der Quantenmechanik (Berlin: Springer)
- [28] Banks T, Susskind L and Kogut J 1976 Strong-coupling calculations of lattice gauge theories: (1 + 1)-dimensional exercises *Phys. Rev.* D 13 1043
- [29] Nagele C, Cejudo J E, Byrnes T and Kleban M 2019 Flux unwinding in the lattice Schwinger model Phys. Rev. D 99 094501
- [30] Bures D 1969 An extension of Kakutani's theorem on infinite product measures to the tensor product of semifinite w*-algebras Trans. Amer. Math. Soc. 135 199
- [31] Uhlmann A 1976 The transition probability in the state space of a *-algebra Rep. Math. Phys. 9 273
- [32] Jozsa R 1994 Fidelity for mixed quantum states J. Mod. Opt. 41 2315
- [33] Katsnelson M I, Dobrovitski V V and Harmon B N 2000 Propagation of local decohering action in distributed quantum systems Phys. Rev. A 62 022118
- [34] Liu H and Suh S J 2014 Entanglement growth during thermalization in holographic systems *Phys. Rev.* D **89** 066012
- [35] Casini H, Liu H and Mezei M 2016 Spread of entanglement and causality J. High Energy Phys. 2016 77